

Relaxation of a two-species magnetofluid and application to finite- β flowing plasmas

L. C. Steinhauer^{a)}

Redmond Plasma Physics Laboratory, University of Washington, Seattle, Washington 98195-2250

A. Ishida

Department of Environmental Science, Faculty of Science, Niigata University, Ikarashi, Niigata 950-21, Japan

(Received 11 November 1997; accepted 26 March 1998)

The relaxation theory of a two-species magnetofluid is presented. This generalizes the familiar magnetohydrodynamic (single-fluid) theory. The two-fluid invariants are the self-helicities, one for each species. Their ‘‘local’’ invariance follows from the helicity transport equations, which are derived. The global forms of the self-helicities are examined in a weakly dissipative system. They are shown to pass three tests of ruggedness (‘‘relative’’ invariance compared with the magnetofluid energy): the cascade test; the selective decay test; and the stability to resistive modes test. Once ruggedness is established, relaxed states can be found by minimizing the magnetofluid energy subject to constrained self-helicities. The Euler equations are found by a variational procedure. Example equilibria are presented that resemble field-reversed configurations (FRCs) and tokamaks. These states are characterized by finite pressure and significant sheared flows. Throughout the analysis it is shown how this more general theory reduces to the magnetohydrodynamic (single-fluid) theory for suitable reducing assumptions. © 1998 American Institute of Physics. [S1070-664X(98)00407-8]

I. INTRODUCTION

Magnetofluids are often observed to self-organize into preferred ‘‘relaxed’’ states (see review in Ref. 1). Such relaxations are interesting because they preserve certain global properties (the ‘‘invariants’’) rather than simply dissipating the magnetic field. This ordered outcome follows despite the complexity and seemingly chaotic nature of the relaxation itself. The relaxation theory based on invariant magnetic helicity^{2,3} has had spectacular success in predicting the gross evolution and structure of reversed-field pinch (RFP) and spheromak plasmas. However, it has had less success predicting tokamak behavior and does not apply at all to field-reversed configurations (FRC). Missing from this theory are such nearly ubiquitous features as finite plasma pressure and significant flow. These shortcomings indicate the theory’s incompleteness and need for extension.

We present a more general relaxation theory based on a two-species (ion and electron) magnetofluid.⁴ The new theory synthesizes familiar concepts: the relaxation of a magnetofluid; the two-fluid model of a magnetofluid; canonical momenta; helicities as invariants; and characteristic ‘‘integral’’ curves of the invariants. This formulation is more realistic than the magnetohydrodynamic (MHD, single-fluid) model on which the previous theory was based. The following argument offers motivation for adopting the two-fluid model. Magnetofluid relaxations proceed by reconnections in very thin layers. However, single-fluid behavior only applies for length scales larger than the collisionless skin depth. On

the small scales in reconnection layers, the ion and electron responses decouple so that the two-fluid treatment is needed. Thus although the MHD theory may capture some aspects of relaxation, it will fail to predict others.

The invariants of a multispecies magnetofluid are the self-helicities,⁵⁻⁹

$$K_\alpha = (c^2/8\pi q_\alpha^2) \int d\tau \mathbf{P}_\alpha \cdot \boldsymbol{\Omega}_\alpha, \quad (1)$$

where $d\tau$ is a volume increment; and the integral is over the entire system volume. These are composite helicities, combining fluid and field behavior through the canonical momentum and the generalized vorticity:

$$\mathbf{P}_\alpha = m_\alpha \mathbf{u}_\alpha + q_\alpha \mathbf{A}/c, \quad \boldsymbol{\Omega}_\alpha = \nabla \times \mathbf{P}_\alpha. \quad (2)$$

Here \mathbf{A} is the vector potential of the fields, and each species (denoted by index α) has the charge, mass, density, pressure, and flow velocity, q_α , m_α , n_α , p_α , \mathbf{u}_α , respectively. The dimensional constant, $c^2/8\pi q_\alpha^2$, is chosen to give K_α energy-length units. The self-helicities have been proposed as invariants elsewhere.⁵⁻⁸ They are related to ‘‘hybrid’’ invariants (that link fluid and field elements): the cross helicity;^{10,11} $K_x = \int \mathbf{u} \cdot \mathbf{B} d\tau$ ($\mathbf{B} = \nabla \times \mathbf{A}$ is the magnetic field), and¹² $\int \mathbf{u} \cdot \boldsymbol{\Omega}_i d\tau$. The well-known simple helicities are the magnetic^{2,10,12-14} $K_m = \int \mathbf{A} \cdot \mathbf{B} d\tau$ and kinetic¹⁰ $K_k = \int \mathbf{u} \cdot \boldsymbol{\omega} d\tau$ ($\boldsymbol{\omega} = \nabla \times \mathbf{u}$ is the fluid vorticity). There is an obvious resemblance between the self- and some of the other helicities: for massless electrons, K_e is equivalent to K_m ; and K_i [expanding Eq. (1), and identifying $\mathbf{u} = \mathbf{u}_i$] is a particular linear sum of the simple helicities. Indeed the two-fluid theory connects the simpler theories of Taylor² (MHD) and Moffatt¹⁰ (non-

^{a)}Electronic mail: steinhauer@aa.washington.edu

TABLE I. Relationship of relaxation theories.

	Fluid (nonmagnetic)	Two-species magnetofluid	MHD (single fluid)
Limits	$\beta \rightarrow \infty$	arbitrary β	$\beta \rightarrow 0$
Local invariants	kinetic helicity, $\mathbf{u} \cdot \nabla \times \mathbf{u}$	self-helicities, $\mathbf{P}_\alpha \cdot \nabla \times \mathbf{P}_\alpha$	magnetic helicity, $\mathbf{A} \cdot \nabla \times \mathbf{A}$
Integral curves (tangential to)	vortex lines, $\boldsymbol{\omega} = \nabla \times \mathbf{u}$	generalized vortex lines, $\boldsymbol{\Omega}_\alpha = \nabla \times \mathbf{P}_\alpha$	magnetic field lines, $\mathbf{B} = \nabla \times \mathbf{A}$
Global invariants	K_k	$\leftarrow K_i, K_e \rightarrow$	K_m
Minimized energy	W_f	$W_{mf} = W_f + W_m$	W_m
Cascade	normal	inverse	inverse

magnetized fluid) as illustrated in Table I. Indeed, the simpler theories are reductions of the more general two-species theory. Stated another way, the two-species theory forms a bridge between the simpler theories. Some properties shown in Table I will be explained later.

We briefly preview the remainder of the paper. Four important questions must be answered in a new relaxation theory: (1) what are the basic invariants in the ideal system; (2) are the global forms of these invariants rugged (relatively durable) in the presence of weak dissipation; (3) what are the corresponding relaxed states; and (4) do the relaxations and the resulting equilibria predict experimental observations?

Section II addresses the first question. Beginning from Maxwell's equations and the equations of motion for each species we derive the helicity transport equations, which govern the local evolutions of the helicities. Each local helicity is associated with infinitesimal bundles of integral curves ("lines of force") that convect with a particular species. The derivation clearly delineates the difference between the MHD and two-fluid models by explicitly displaying the electromechanical coupling (Lorentz) force, the vanishing of which is assumed in ideal MHD. The cancellation of the Lorentz force in the self-helicity transport equations indicates that the self-helicities are natural two-fluid invariants. As such, two-fluid relaxation bridges the gap between previous theories for limiting cases (pure fluid; magnetized, current carrying medium) as shown in Table I. We also derive a circulation theorem for the self-helicities.

Section III addresses the second question. Although the existence of local helicities is a necessary basis, even weak dissipations unleash processes that compromise the identity of local helicities. Only the global form of helicity is safe from topology changes. However, even then it is not assured that a global helicity will be robust in the presence of non-linear turbulence. Consideration of this question calls for a quasilinear analysis of wave processes with which tests of invariance can be made (Sec. III A). Here we introduce the electromechanical coupling operators as devices for expressing the fluid-field coupling. A selection takes place on the basis of the wave energy: this selection is not only between like waves with a different wave number, but also between waves of different type. The energetically favorable wave type in a two-fluid is the *R* wave (whistler wave in the higher frequency range). We apply each of three ruggedness tests: *inverse cascade* (Sec. III B), which is necessary for relaxation toward larger-scale objects; *selective decay* (Sec. III C),

which tests whether a helicity invariant is more durable than the magnetofluid energy; and *stability to resistive modes* (Sec. III B), which tests whether a helicity decays more slowly than the reconnection rate. In MHD the magnetic helicity passes these tests while the cross and kinetic helicities fail. In a two fluid, both self-helicities pass these tests. Importantly, although the ion self-helicity is rugged in the two-fluid model, the MHD model fails to capture this property.

Section IV addresses the third question. Global invariants that survive the relaxation are suitable constraints in an energy minimization. This procedure leads to three Euler equations governing the relaxed state: two flow equations (one for each species) and an equation equivalent to Ampere's law. This system of equations is closed by adding the steady equation of motion, which takes the form of a Bernoulli equation linking the pressure and flow speed. In the reduced case of MHD (no ion self-helicity invariant) the electron flow equation reverts to the familiar force-free condition.

Section V addresses the fourth question. Assuming one-dimensional geometric analogies it is straightforward to find example relaxed states. Force-free states (included in the two-fluid theory) are well known. We present FRC and tokamak examples, which are clearly outside the scope of MHD relaxation theory. The FRC example resembles laboratory plasmas, exhibiting *high* β , no "toroidal" magnetic field, hollow current profile, significant rotational flow, and a natural plasma edge with thickness comparable to an ion gyroradius. The tokamak example resembles the core of reversed-magnetic shear experiments, exhibiting reversed magnetic shear, hollow current profile, and high flow speed. These examples represent aspects of qualitative agreement between the theory and experiment. A more detailed, quantitative confirmation awaits future work. The paper concludes (Sec. VI) with a discussion.

II. INVARIANTS OF ONE- AND TWO-SPECIES MAGNETOFLUIDS

A. Helicity transport equations

The *global* invariance was shown for the magnetic helicity,^{11,13} the kinetic¹⁰ and cross helicities,^{10,15} and the ion self-helicity^{5,6,8,9} in the ideal (dissipationless) case. However, global invariants must have a local basis, i.e., global invariance must spring from some principle of the local evolution of a particular quadratic quantity. (For example, a local basis

has *not* been established for the frugidity¹⁶). Note that “local” is a two-dimensional designation since it applies to integral curves in three-dimensional space. The equation governing the evolution of a local helicity has been called the helicity transport equation.¹⁷ Such equations have been found for the kinetic helicity¹⁰ and the magnetic helicity.^{17–19} Here we present the first derivation of the transport equations for the self-helicities. To clarify the distinction between the MHD and the two-fluid model we adopt the following approach: (a) begin from a multispecies magnetofluid paradigm in a form that explicitly shows the electromechanical coupling force; (b) derive expressions for the evolution of vector quantities referenced to a particular species; (c) combine these into suitable quadratic invariants (helicity transport equations); and finally (d) find local and global invariants in the dissipationless case for both MHD and a multispecies magnetofluid.

The starting point is the multispecies magnetofluid description (originally suggested by Sudan¹²) where each pressure is scalar and a function of the density, $p_\alpha = p_\alpha(n_\alpha)$, i.e., the barotropic assumption. We will arrange the basic equations (Maxwell’s equations, equations of motion) in forms that (a) reference the evolution to a particular species by using the total derivative, $D_\alpha/Dt = \partial/\partial t + \mathbf{u}_\alpha \cdot \nabla$ (following Moffatt¹⁰); and (b) replace the electric field in favor of the Lorentz force on a particle of species α :

$$\mathbf{F}_\alpha = q_\alpha(\mathbf{E} + \mathbf{u}_\alpha \times \mathbf{B}/c), \tag{3}$$

where \mathbf{E} and \mathbf{B} are the electric and magnetic fields, and c is the speed of light in vacuum. The Lorentz force is the electromechanical coupling force. Note that the simplified form of Ohm’s law for ideal MHD is simply $\mathbf{F}_i = 0$, i.e., no direct electromechanical coupling between the field and ions.

We express the evolution of fluid and field quantities as companion pairs of equations: the first in each pair expresses the evolution of a vector quantity; and its companion expresses the evolution of the *curl* of that vector. Consider first the electric field expressed in terms of the potentials, \mathbf{A} and ϕ : $\mathbf{E} = -\nabla\phi - (1/c)\partial\mathbf{A}/\partial t$. Modify this to construct the total derivative (add $\mathbf{u}_\alpha \cdot \nabla\mathbf{A}$ to both sides); and replace \mathbf{E} in favor of the Lorentz force using Eq. (3). Then

$$\frac{D_\alpha \mathbf{A}}{Dt} = \mathbf{u}_\alpha \times \mathbf{B} + \mathbf{u}_\alpha \cdot \nabla \mathbf{A} - c \nabla \phi - \frac{c}{q_\alpha} \mathbf{F}_\alpha. \tag{4}$$

The companion field equation arises from Faraday’s law, $\partial\mathbf{B}/\partial t = -c \nabla \times \mathbf{E}$. Augment this (as before) to express the total derivative; subtract \mathbf{B} times a form of the continuity equation [$(1/n_\alpha)D_\alpha n_\alpha/Dt = \nabla \cdot \mathbf{u}_\alpha$]; eliminate \mathbf{E} by Eq. (3); and simplify with the identity $\nabla \times (\mathbf{u}_\alpha \times \mathbf{B}) = \mathbf{u}_\alpha \nabla \cdot \mathbf{B} - \mathbf{B} \nabla \cdot \mathbf{u}_\alpha + \mathbf{B} \cdot \nabla \mathbf{u}_\alpha - \mathbf{u}_\alpha \cdot \nabla \mathbf{B}$, recognizing $\nabla \cdot \mathbf{B} = 0$. Then

$$n_\alpha \frac{D_\alpha}{Dt} \left(\frac{\mathbf{B}}{n_\alpha} \right) = \mathbf{B} \cdot \nabla \mathbf{u}_\alpha - \frac{c}{q_\alpha} \nabla \times \mathbf{F}_\alpha. \tag{5}$$

Consider next the pair of equations for the fluid motion. Using the barotropic function, $h_\alpha \equiv \int dp_\alpha/m_\alpha n_\alpha$, the equation of motion for species α is

$$m_\alpha \frac{D_\alpha \mathbf{u}_\alpha}{Dt} = -m_\alpha \nabla h_\alpha + \mathbf{F}_\alpha + \frac{\mathbf{R}_\alpha}{n_\alpha}, \tag{6}$$

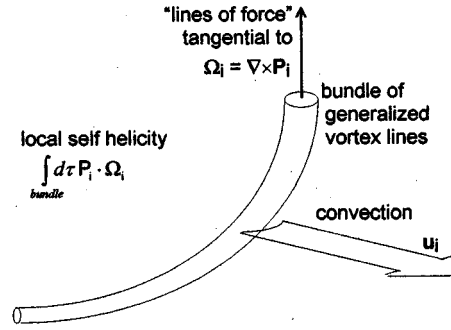


FIG. 1. Generalized vortex line and local self-helicity for ions.

where \mathbf{R}_α is the friction force density. The companion equation governing $\boldsymbol{\omega}_\alpha = \nabla \times \mathbf{u}_\alpha$, the fluid vorticity, is found as follows: expand the convective term in the total derivative $D_\alpha u_\alpha/Dt$ using the identity $\mathbf{u} \cdot \nabla \mathbf{u} = \nabla(u^2/2) - \mathbf{u} \times (\nabla \times \mathbf{u})$; take the curl of the resulting equation; augment $\partial\boldsymbol{\omega}_\alpha/\partial t$ to construct the total derivative; add $\boldsymbol{\omega}_\alpha$ times a form of the continuity equation; and simplify with the identity, $\nabla \times (\mathbf{u}_\alpha \times \boldsymbol{\omega}_\alpha) = \mathbf{u}_\alpha \nabla \cdot \boldsymbol{\omega}_\alpha - \boldsymbol{\omega}_\alpha \nabla \cdot \mathbf{u}_\alpha + \boldsymbol{\omega}_\alpha \cdot \nabla \mathbf{u}_\alpha - \mathbf{u}_\alpha \cdot \nabla \boldsymbol{\omega}_\alpha$ recognizing $\nabla \cdot \boldsymbol{\omega}_\alpha = 0$. Then

$$m_\alpha n_\alpha \frac{D_\alpha}{Dt} \left(\frac{\boldsymbol{\omega}_\alpha}{n_\alpha} \right) = m_\alpha \boldsymbol{\omega}_\alpha \cdot \nabla \mathbf{u}_\alpha + \nabla \times \mathbf{F}_\alpha + \nabla \times \left(\frac{\mathbf{R}_\alpha}{n_\alpha} \right). \tag{7}$$

Finally, consider a pair of equations that combine a fluid species and the fields to form the canonical momentum, and its companion the generalized vorticity, Eq. (2). The evolution of \mathbf{P}_α follows from combining $q_\alpha/c \cdot [\text{Eq. (4)}] + \text{Eq. (6)}$:

$$\frac{D_\alpha \mathbf{P}_\alpha}{Dt} = \frac{q_\alpha}{c} (\mathbf{u}_\alpha \times \mathbf{B} + \mathbf{u}_\alpha \cdot \nabla \mathbf{A}) - \nabla (m_\alpha h_\alpha + q_\alpha \phi) + \frac{\mathbf{R}_\alpha}{n_\alpha}. \tag{8}$$

Its companion follows from combining $q_\alpha/c \cdot [\text{Eq. (5)}] + \text{Eq. (7)}$:

$$n_\alpha \frac{D_\alpha}{Dt} \left(\frac{\boldsymbol{\Omega}_\alpha}{n_\alpha} \right) = \boldsymbol{\Omega}_\alpha \cdot \nabla \mathbf{u}_\alpha + \nabla \times \left(\frac{\mathbf{R}_\alpha}{n_\alpha} \right). \tag{9}$$

This equation for the evolution of $\boldsymbol{\Omega}_\alpha$ is preferable to those derived earlier^{5,6} in that it references the evolution to a particular species. Equation (9) implies that generalized vortex lines convect with the species, as is illustrated for the ion fluid in Fig. 1. That the ion generalized vortex lines convect with the ion fluid was suggested by Turner.⁶ The Appendix gives a proof of this for either species. Summarizing, we have three pairs of equations [Eqs. (4)–(9)] governing the evolution of the quantities, \mathbf{A} , \mathbf{u}_α , and \mathbf{P}_α and their “specific” curl forms \mathbf{B}/n_α , $\boldsymbol{\omega}_\alpha/n_\alpha$, and $\boldsymbol{\Omega}_\alpha/n_\alpha$ (specific meaning *per particle*). [The third pair, Eqs. (8) and (9), are linearly dependent on the other two.] In each case the evolution is referenced to a species using the total derivative. In two pairs the electromechanical coupling (Lorentz force, \mathbf{F}_α) ap-

pears explicitly. Significantly, in the third pair \mathbf{F}_α is absent, suggesting that \mathbf{P}_α and $\mathbf{\Omega}_\alpha/n_\alpha$ express the natural fluid-field coupling.

The next step is to combine these equations to find expressions for quadratic elements, the local helicities, which are candidates for invariance. The specific forms of these are $u_\alpha \cdot \boldsymbol{\omega}_\alpha/n_\alpha$ (kinetic helicity); $\mathbf{A} \cdot \mathbf{B}/n_\alpha$ (magnetic helicity); $u_\alpha \cdot \mathbf{B}/n_\alpha$ (cross helicity); and $\mathbf{P}_\alpha \cdot \mathbf{\Omega}_\alpha/n_\alpha$ (self-helicity). The results might be called helicity transport equations,¹⁶ which have been derived for the kinetic,¹⁰ magnetic,^{10,17-19} and cross helicities.¹⁰ The kinetic helicity transport equation arises as follows: construct $\boldsymbol{\omega}_\alpha \cdot$ [Eq. (6)] + $\mathbf{u}_\alpha \cdot$ [Eq. (7)]; simplify with the identity $\mathbf{u}_\alpha \cdot (\boldsymbol{\omega}_\alpha \cdot \nabla \mathbf{u}_\alpha) = \boldsymbol{\omega}_\alpha \cdot \nabla u_\alpha^2/2$; and “integrate by parts” the $\nabla \times \mathbf{F}_\alpha$, $\nabla \times (\mathbf{R}_\alpha/n_\alpha)$, and $\boldsymbol{\omega}_\alpha \cdot \nabla(\dots)$ terms. Then

$$m_\alpha n_\alpha \frac{D_\alpha}{Dt} \left(\frac{\mathbf{u}_\alpha \cdot \boldsymbol{\omega}_\alpha}{n_\alpha} \right) = \nabla \cdot \left[m_\alpha \left(\frac{u_\alpha^2}{2} - h_\alpha \right) \boldsymbol{\omega}_\alpha + \mathbf{u}_\alpha \times \mathbf{F}_\alpha + \frac{\mathbf{R}_\alpha}{n_\alpha} \times \mathbf{u}_\alpha \right] + 2\mathbf{u}_\alpha \cdot \nabla \times \mathbf{F}_\alpha + 2\mathbf{u}_\alpha \cdot \nabla \times \left(\frac{\mathbf{R}_\alpha}{n_\alpha} \right). \tag{10}$$

The magnetic helicity transport equation is found as follows: construct $\mathbf{B} \cdot$ [Eq. (4)] + $\mathbf{A} \cdot$ [Eq. (5)]; simplify with the identity $\mathbf{A} \cdot (\mathbf{B} \cdot \nabla \mathbf{u}_\alpha) = \mathbf{B} \cdot \nabla (\mathbf{u}_\alpha \cdot \mathbf{A}) - \mathbf{B} \cdot (\mathbf{u}_\alpha \cdot \nabla \mathbf{A})$; integrate by parts on the $\nabla \times \mathbf{F}_\alpha$ and $\mathbf{B} \cdot \nabla(\dots)$ terms, recognizing that $\nabla \cdot \mathbf{B} = 0$. Then

$$n_\alpha \frac{D_\alpha}{Dt} \left(\frac{\mathbf{A} \cdot \mathbf{B}}{n_\alpha} \right) = -\nabla \cdot \left[(c\phi - \mathbf{u}_\alpha \cdot \mathbf{A}) \mathbf{B} + \frac{c}{q_\alpha} \mathbf{A} \times \mathbf{F}_\alpha \right] - 2 \frac{c}{q_\alpha} \mathbf{A} \cdot \nabla \times \mathbf{F}_\alpha. \tag{11}$$

The cross helicity transport equation is found as follows: construct $m_\alpha \mathbf{u}_\alpha \cdot$ [Eq. (5)] + $\mathbf{B} \cdot$ [Eq. (6)]; and integrate by parts the $\nabla \times \mathbf{F}_\alpha$ and $\mathbf{B} \cdot \nabla(\dots)$ terms. Then

$$m_\alpha n_\alpha \frac{D_\alpha}{Dt} \left(\frac{\mathbf{u}_\alpha \cdot \mathbf{B}}{n_\alpha} \right) = \nabla \cdot \left[m_\alpha \left(\frac{u_\alpha^2}{2} - h_\alpha \right) \mathbf{B} + \frac{m_\alpha c}{q_\alpha} \mathbf{u}_\alpha \times \mathbf{F}_\alpha \right] + \frac{c}{q_\alpha} \mathbf{F}_\alpha \cdot \left[\nabla \times \left(\frac{q_\alpha \mathbf{A}}{c} - m_\alpha \mathbf{u}_\alpha \right) \right] + \mathbf{B} \cdot \frac{\mathbf{R}_\alpha}{n_\alpha}. \tag{12}$$

The transport equations for the self-helicities are found as follows: construct $\mathbf{\Omega}_\alpha \cdot$ [Eq. (8)] + $\mathbf{P}_\alpha \cdot$ [Eq. (9)]; simplify with the identity $\mathbf{P}_\alpha \cdot (\mathbf{\Omega}_\alpha \cdot \nabla \mathbf{u}_\alpha) = \mathbf{\Omega}_\alpha \cdot \nabla (\mathbf{P}_\alpha \cdot \mathbf{u}_\alpha) - \mathbf{\Omega}_\alpha \cdot (\mathbf{u}_\alpha \cdot \nabla \mathbf{P}_\alpha)$; substitute $\mathbf{P}_\alpha = m_\alpha \mathbf{u}_\alpha + q_\alpha \mathbf{A}/c$; expand $\mathbf{u}_\alpha \cdot \nabla \mathbf{u}_\alpha = \nabla u_\alpha^2/2 - \mathbf{u}_\alpha \times \nabla \mathbf{u}_\alpha$; and integrate by parts on the $\mathbf{\Omega}_\alpha \cdot \nabla(\dots)$ and $(\nabla \times \mathbf{P}_\alpha) \cdot \mathbf{R}_\alpha$ terms. Then

$$n_\alpha \frac{D_\alpha}{Dt} \left(\frac{\mathbf{P}_\alpha \cdot \mathbf{\Omega}_\alpha}{n_\alpha} \right) = \nabla \cdot \left[\left(\mathbf{u}_\alpha \cdot \mathbf{P}_\alpha - \frac{1}{2} m_\alpha u_\alpha^2 - m_\alpha h_\alpha - q_\alpha \phi \right) \mathbf{\Omega}_\alpha - \mathbf{P}_\alpha \times \frac{\mathbf{R}_\alpha}{n_\alpha} \right] + 2\mathbf{\Omega}_\alpha \cdot \frac{\mathbf{R}_\alpha}{n_\alpha} \tag{13}$$

Physically, the self-helicities represent a measure of the self-linkage, or knottedness, of the generalized vorticity.⁶ Summarizing, we have four helicity transport equations, Eqs. (10)–(13). Each references the evolution to a particular species using the total derivative. Each right side is the sum of a divergence term, and force terms for the friction ($\mathbf{R}_\alpha/n_\alpha$) and the electromechanical coupling \mathbf{F}_α . In the event that the divergence operates on a scalar times a vector, then the vectors define integral curves or “lines of force” associated with the helicity.

B. Local and global invariance concepts

1. Local invariance

With the helicity transport equations in hand we can now address the concept of local invariance in the “ideal” case ($\mathbf{R}_\alpha = 0$). Local invariance is related to families of integral curves defined by the divergence terms in the helicity transport equations, Eqs. (11)–(13). Consider the local self-helicity. Define a volume defined as a tube of generalized vorticity (bundle of generalized vorticity lines), so that at its surface $\mathbf{\Omega}_\alpha$ is tangential to the surface. Suppose further that the bundle nowhere intercepts the system boundary. Integrate Eq. (13) over this volume. From continuity, $D_\alpha(n_\alpha d\tau)/Dt = 0$, so the left side becomes $(d/dt) \int d\tau \mathbf{P}_\alpha \cdot \mathbf{\Omega}_\alpha$, which is the rate of change of the “local” helicity associated with the bundle. The right side (with $\mathbf{R}_\alpha = 0$) is the integral of the divergence of a vector tangential to $\mathbf{\Omega}_\alpha$; using Gauss’s theorem this converts to a surface integral $\int (\dots) \mathbf{\Omega}_\alpha \cdot d\mathbf{S}$, where $d\mathbf{S}$ is an incremental area element on the surface of the bundle. Since $\mathbf{\Omega}_\alpha$ is tangential to the surface, then $\mathbf{\Omega}_\alpha \cdot d\mathbf{S} = 0$, and the surface integral vanishes. Therefore, the local helicity associated with the bundle of generalized vorticity is constant:

$$(K_\alpha)_{\text{bundle}} \equiv \frac{c^2}{8\pi q_\alpha^2} \int_{\text{bundle}} d\tau \mathbf{P}_\alpha \cdot \mathbf{\Omega}_\alpha = \text{const.} \tag{14}$$

This concept of local invariance is illustrated for the ion fluid in Fig. 1. The constancy of $(K_\alpha)_{\text{bundle}}$ implies that the local ion self-helicity is “frozen in” a bundle of generalized vortex lines.⁶ Note that if a field line is ergodic it fills up a surface; in this case local invariance is associated with surfaces rather than lines. The electron self-helicity is similar except that it is frozen to generalized electron vortex lines and convects with the electron fluid. Consider next MHD, which is the reduced case for a single fluid ($\alpha = i$). Here the simplified form of Ohm’s law is $\mathbf{F}_i = 0$. Then in each of the transport equations for the three simple helicities [Eqs. (10)–(12)], the right sides become divergences of a scalar times the vector which defines the lines of force. By the same procedures as before it follows that the local helicities associated with the respective bundles is constant.

2. Circulation theorems

The local helicities are closely related to the concept of circulation. Define the generalized circulation of species α as

$$\Gamma_\alpha(C_{\Omega_\alpha}) \equiv \oint_{C_{\Omega_\alpha}} \mathbf{P}_\alpha \cdot d\mathbf{x}, \tag{15}$$

where C_{Ω_α} is a closed curve lying entirely within the system volume enclosing a specified bundle of generalized vorticity lines, and $d\mathbf{x}$ is an incremental length vector along C_{Ω_α} . The rate of change $d\Gamma_\alpha/dt$ is then the integral of two terms, $D_\alpha \mathbf{P}_\alpha / Dt$ [given by Eq. (8), taking $\mathbf{R}_\alpha = 0$ in the ideal case] and $\mathbf{P}_\alpha \cdot (D_\alpha / Dt) d\mathbf{x}$. In the latter expand $\mathbf{P}_\alpha = m_\alpha \mathbf{u}_\alpha + q_\alpha \mathbf{A} / c$ and use $(D_\alpha / Dt) d\mathbf{x} = d\mathbf{x} \cdot \nabla \mathbf{u}_\alpha$. Then with the identity, $\nabla(\mathbf{u} \cdot \mathbf{A}) = \mathbf{u} \times (\nabla \times \mathbf{A}) + \mathbf{A} \times (\nabla \times \mathbf{u}) + \mathbf{u} \cdot \nabla \mathbf{A} + (\nabla \mathbf{u}) \cdot \mathbf{A}$, the rate of change simplifies to

$$\begin{aligned} \frac{d\Gamma_\alpha(C_{\Omega_\alpha})}{dt} &= \oint_{C_{\Omega_\alpha}} d\mathbf{x} \cdot \nabla \left(\mathbf{u}_\alpha \cdot \mathbf{A} - m_\alpha h_\alpha + \frac{1}{2} m_\alpha u_\alpha^2 - q_\alpha \phi \right) \\ &= 0. \end{aligned} \tag{16}$$

The vanishing is the result of integrating a gradient of a well-behaved function around a closed loop. Thus in the ideal case the generalized circulation associated with a curve convecting with species α is constant. In ideal MHD, a similar procedure shows the invariance of the associated circulations, $\Gamma_K(C_\omega) = \oint_{C_\omega} d\mathbf{x} \cdot \mathbf{u}$, $\Gamma_X(C_B) = \oint_{C_B} d\mathbf{x} \cdot \mathbf{u}$, and $\Gamma_m(C_B) = \oint_{C_B} d\mathbf{x} \cdot \mathbf{A}$, where C_ω , C_B are closed curves enclosing specified bundles of fluid vorticity and magnetic field lines, respectively. Note that the integrands of Γ_K and Γ_X are the same, but are integrated on curves with a different identity.

3. Failure of local invariance

In the ideal case the lines of force cannot break or coalesce so that their topological properties, e.g., their helicities, are preserved.² However, real plasmas are not perfectly ideal, having frictional forces, \mathbf{R}_α arising from the resistivity η , and viscosity coefficient ν . Unfortunately the convergence is nonuniform so that the ideal case ($\eta, \nu = 0$) leads to markedly different results than the weakly dissipative case ($0 \neq \eta, \nu \ll 1$).^{2,3,20} Indeed, as $\eta, \nu \rightarrow 0$ the regions over which dissipation acts merely get smaller and the gradients correspondingly large: the rate at which lines of force reconnect does not decrease as fast as η, ν , and may not decrease at all. Reconnection causes the individual lines of force to lose their identity.^{3,7}

4. Global invariance

Reconnections juggle helicity information between the lines of force. However, for proper surface conditions (Ω_α and \mathbf{u}_α not intersecting the boundary) then the global helicity $K_\alpha \sim \int \mathbf{P}_\alpha \cdot \Omega_\alpha d\tau$ remains the same, i.e., the global invariance is independent of interior topological changes. This follows by a procedure analogous to that which led to Eq. (14) except using the system volume rather than the ‘‘bundle’’ volume. Then global invariance relies on the vanishing normal component $(\Omega_\alpha)_n = \Omega_\alpha \cdot \hat{\mathbf{n}}$ at the boundary. If initially $(\Omega_\alpha)_n = 0$ everywhere on the boundary, and there is no flow

through the boundary, $\mathbf{u}_\alpha \cdot \hat{\mathbf{n}} = 0$, then $(\Omega_\alpha)_n$ will always remain zero in the ideal (frictionless) case. This is proved using the normal component of Eq. (9) divided by n_α . For no normal flow the left side is $\partial[(\Omega_\alpha)_n / n_\alpha] / \partial t$. Initially both Ω_α / n_α and \mathbf{u}_α only have tangential components at the boundary, the right side vanishes. Therefore $(\Omega_\alpha)_n / n_\alpha$ will not change from its initial zero value. The introduction of dissipation affects the preservation of the helicities not only at the boundary but throughout the region. Whether K_α (and in MHD, K_K, K_X, K_m) are adequately preserved in the weakly dissipative case is taken up in the next section.

III. RUGGEDNESS OF INVARIANTS IN TURBULENT MAGNETOFLUIDS

A. Electromechanical coupling

In order for helicity invariants to play a role in defining relaxed states, they must be rugged, i.e., in a relaxation they must be more durable than the magnetofluid energy, which is the sum of flow kinetic, magnetic, and electrostatic energies:^{6,7,10,21}

$$W_{mf} = \int d\tau \left(\frac{1}{2} \sum_\alpha m_\alpha n_\alpha u_\alpha^2 + \frac{B^2}{8\pi} + \frac{E^2}{8\pi} \right). \tag{17}$$

Accordingly, a useful relaxation theory rests on three requirements, which might be called ‘‘ruggedness tests’’ for the invariants: (1) *inverse cascade*, the ‘‘direction’’ of the relaxation must be toward larger size structures; (2) *selective decay*, the helicity invariant must decay more slowly than the magnetofluid energy; and (3) *stability to resistive modes*, the helicity must be stable to resistive modes, i.e., the time scale for topology change must be faster than that for change in the helicity. These three tests have previously been applied to the magnetic helicity.^{3,20–23} Applying these to the self-helicities is more difficult since (unlike with K_M), the fluid-field coupling cannot be ignored. For this we adopt the well-known paradigm of quasilinear theory, i.e., that the frequencies and responses of linear theory are retained even though some waves will grow to nonlinear amplitudes. We apply the three tests of ruggedness in Secs. III B, C, and D. Our analysis ignores electron inertia, which excludes high-frequency phenomena (plasma frequency, electron cyclotron frequency) and assures quasineutrality, $n_i = n_e = n$, and also makes the electrostatic energy density, $E^2 / 8\pi$, negligible. Hereafter we use the subscripts i and e to refer to ions and electrons, when expressions are used that specifically apply to one species but not the other. These simplifications are identical to what is known as *incompressible Hall MHD*.²⁴

The fluid medium and the fields are combined in the magnetofluid energy and in some of the helicities. The first step then is to establish the fluid-field coupling. All perturbed quantities are Fourier analyzed: e.g., $\mathbf{u}_\alpha \rightarrow \tilde{\mathbf{u}}_\alpha \exp(i\mathbf{k} \cdot \mathbf{r} - i\omega t)$, where ω and \mathbf{k} are the frequency and wave vector of a mode. For simplicity we regard \mathbf{k} as a continuous variable; in a real system with bounded geometry, k assumes discrete values, the smallest of which is set by the system size.^{8,25} Consider for now a nondrifting, cold, magnetized plasma. The equations of motion in terms of the vector potential are

$$m_\alpha \tilde{\mathbf{u}}_\alpha = \mp (|q_\alpha|/c) \tilde{\mathbf{A}} \pm i(\omega_{c\alpha}/\omega) m_\alpha \tilde{\mathbf{u}}_\alpha \times \mathbf{b}, \quad (18)$$

where the gyrofrequencies, $\omega_{c\alpha} = |q_\alpha| B_0 / m_\alpha c$, are positive numbers; the upper (lower) signs denote ions (electrons); $\mathbf{b} \equiv \mathbf{B}_0 / B_0$, and the subscript 0 denotes the ambient quantity. The mechanical response to the fields can be expressed using an electromechanical coupling operator $\vec{\sigma}_\alpha$:

$$m_\alpha \tilde{\mathbf{u}}_\alpha = \vec{\sigma}_\alpha \cdot (q_\alpha \tilde{\mathbf{A}} / c). \quad (19)$$

These are more useful than the conventional dielectric function,²⁶ $\vec{\epsilon}$, since they distinguish the mechanical responses of each species. Suppose that the equilibrium magnetic field is in the z direction. Then

$$\vec{\sigma}_\alpha = \begin{bmatrix} \sigma_{\alpha 1} & i\sigma_{\alpha 2} & 0 \\ -i\sigma_{\alpha 2} & \sigma_{\alpha 1} & 0 \\ 0 & 0 & -1 \end{bmatrix}, \quad (20)$$

where

$$\sigma_{\alpha 1} = \omega^2 / (\omega_{c\alpha}^2 - \omega^2), \quad (21a)$$

$$\sigma_{\alpha 2} = \pm \omega_{c\alpha} \omega / (\omega_{c\alpha}^2 - \omega^2). \quad (21b)$$

Retaining the mass ratio $\mu = m_i / m_e \gg 1$ as a parameter, these elements are

$$\sigma_{i1} = (\omega / \omega_{ci}) \sigma_{i2} = (\omega / \omega_{ci})^2 [1 - (\omega / \omega_{ci})^2]^{-1}, \quad (22a)$$

$$\sigma_{e1} \approx -(\omega / \omega_{ce}) \sigma_{e2} \approx \mu^{-2} (\omega / \omega_{ci})^2. \quad (22b)$$

1. Dispersion relation

Ampere's law with current density, $\mathbf{j} = \sum q_\alpha n_\alpha \mathbf{u}_\alpha$, and the gauge $\phi = 0$ becomes

$$-\mathbf{k} \times (\mathbf{k} \times \tilde{\mathbf{A}}) = \sum_\alpha \omega_{p\alpha}^2 \frac{m_\alpha \tilde{\mathbf{u}}_\alpha}{q_\alpha c} + \frac{\omega^2}{c^2} \tilde{\mathbf{A}}. \quad (23)$$

In terms of the electromechanical coupling operator [Eq. (19)] this is

$$-\mathbf{k} \times (\mathbf{k} \times \tilde{\mathbf{A}}) = \frac{\omega^2}{c^2} \left[\vec{I} + \sum_\alpha \frac{\omega_{p\alpha}^2}{\omega^2} \vec{\sigma}_\alpha \right] \cdot \tilde{\mathbf{A}}, \quad (24)$$

where $\omega_{p\alpha} = (4\pi q_\alpha^2 n_{\alpha 0} / m_\alpha)^{1/2}$ are the plasma frequencies for $\alpha = i, e$. The term in square brackets is the familiar dielectric function, $\vec{\epsilon}$. Note that unlike $\vec{\epsilon}$, the coupling operators $\vec{\sigma}_\alpha$ distinguish the responses of each species. Equation (24) can be expressed as a matrix times $\tilde{\mathbf{A}}$ equals zero: the vanishing determinant of that matrix is the dispersion relation. Consider two limiting cases when the \mathbf{k} is either parallel or perpendicular to the ambient field. Then the dispersion relations are

$$\text{parallel } (\mathbf{k} \parallel \mathbf{b}): \quad (kl_c)^2 = (\omega / \omega_{ci})^2 [1 \pm \omega / \omega_{ci}]^{-1}, \quad (25)$$

$$\text{perpendicular } (\mathbf{k} \perp \mathbf{b}): \quad (kl_c)^2 = (\omega / \omega_{ci})^2. \quad (26)$$

Here $l_c = c / \omega_{pi}$ is the collisionless skin depth. In the parallel case the upper and lower signs represent right and left polarized (R,L) waves. In the perpendicular case the second root has high frequency (approaching infinity for $\mu \rightarrow \infty$) thus is excluded from this treatment. In deriving Eqs. (25) and (26) we assumed $\omega_{pi} / \omega_{ci} \approx 0$ (Alfvén speed/speed of light), as

generally holds in fusion-relevant plasmas. Evidently, when high-frequency phenomena are excluded, the natural length (as shown by Turner⁶) and frequency scales are l_c and ω_{ci} , respectively.

2. Mechanical responses

In the parallel case the frequency (for R and L waves) is

$$\omega / \omega_{ci} = kl_c [\pm kl_c / 2 + \sqrt{1 + (kl_c)^2 / 4}]$$

and the mechanical responses are

$$m_i \tilde{\mathbf{u}}_i = \frac{\omega / \omega_{ci}}{1 \pm \omega / \omega_{ci}} \frac{e \tilde{\mathbf{A}}}{c}, \quad (27a)$$

$$m_e \tilde{\mathbf{u}}_e = \mp \mu^{-1} (\omega / \omega_{ci}) \frac{e \tilde{\mathbf{A}}}{c}. \quad (27b)$$

The base vector in the parallel case [from Eq. (24)] is $\tilde{\mathbf{A}} = (\hat{\mathbf{x}} \pm i \hat{\mathbf{y}}) \tilde{A} / \sqrt{2}$, and has the property that will be useful later:

$$i \mathbf{k} \cdot (\tilde{\mathbf{A}} \times \tilde{\mathbf{A}}^*) = \pm k_\parallel \tilde{A}^2. \quad (28)$$

For $kl_c < 1$ the responses are Alfvén like, while for $kl_c > 1$ they are the whistler (R) and ion-cyclotron (L) waves. The familiar MHD model assumes that the very low frequency behavior, $\omega / \omega_{ci} = kl_c$, holds for all ranges of k . Note that since $l_c \omega_{ci} = v_{A0} = B_0 / (4\pi m_i n_0)^{1/2}$ (Alfvén speed) this is equivalent to $\omega = kv_A$. Thus the MHD model properly represents low-frequency, low- k phenomena ($\omega \ll \omega_{ci}$, corresponding to $kl_c \ll 1$). It cannot, however, be expected to describe the high- k behavior.

3. Two-fluid energy and helicities

The Fourier-transformed magnetofluid energy for the low-frequency model is

$$\tilde{W}_{mf} = \frac{1}{8\pi} \left(|\mathbf{k} \times \tilde{\mathbf{A}}|^2 + \frac{1}{l_c^2} |\vec{\sigma}_i \cdot \tilde{\mathbf{A}}|^2 \right). \quad (29)$$

This compares with the result from the rigorous procedure using the dielectric function,²⁶ modified to express the coupling operators:

$$\tilde{W}_{mf} = \frac{1}{8\pi} \left\{ \frac{\omega^2}{c^2} \tilde{A}^2 + |\mathbf{k} \times \tilde{\mathbf{A}}|^2 + \frac{\omega^2}{c^2} \sum_\alpha \omega_{p\alpha}^2 \tilde{\mathbf{A}}^* \cdot \frac{d}{d\omega} \left(\frac{\vec{\sigma}_\alpha}{\omega} \right) \cdot \tilde{\mathbf{A}} \right\}. \quad (30)$$

The three terms represent the electric, magnetic, and fluid effects. A tedious but straightforward analysis shows that excluding high-frequency phenomena (negligible electric energy) reduces this to Eq. (29). Using the ion momentum [Eq. (27a)]:

$$\tilde{W}_{mf} = \left[\left(\frac{\omega / \omega_{ci}}{1 \pm \omega / \omega_{ci}} \right)^2 \frac{1}{l_c^2} + k^2 \right] \frac{\tilde{A}^2}{8\pi}. \quad (31)$$

The upper sign applies to the R wave, and the lower sign applies to the L wave and the magnetosonic wave. The Fourier-transformed self-helicity is

$$\tilde{K}_a = \frac{c^2}{4\pi q_\alpha^2} \mathbf{i} \mathbf{k} \cdot (\tilde{\mathbf{P}}_\alpha \times \tilde{\mathbf{P}}_\alpha^*). \quad (32)$$

Using Eq. (2) and the mechanical responses, Eqs. (27a) and (27b) and noting the property of the base vectors, Eq. (28), the self-helicities become

parallel:
$$\tilde{K}_i = \frac{k}{(1 \pm \omega/\omega_{ci})^2} \frac{\tilde{A}^2}{4\pi}, \quad (33a)$$

$$\tilde{K}_e = k \frac{\tilde{A}^2}{4\pi}; \quad (33b)$$

perpendicular:
$$\tilde{K}_i = \tilde{K}_e = 0. \quad (34)$$

Observe that the magnetosonic wave carries self-helicity.

4. MHD energy and helicities

MHD corresponds to the limit $\omega/\omega_{ci} \ll 1$. Then its magnetofluid energy and helicities are

$$\tilde{W}_{mf} = 2k^2 \frac{\tilde{A}^2}{8\pi}, \quad (35a)$$

$$\tilde{K}_m = k\tilde{A}^2, \quad (35b)$$

$$\tilde{K}_x = k^2(e/m_i c)\tilde{A}^2, \quad (35c)$$

$$\tilde{K}_k = k^3(e/m_i c)^2\tilde{A}^2. \quad (35d)$$

Although the self-helicities are not invariant in MHD, it is instructive (as well be shown) to show their forms:

$$\tilde{K}_i = k(1 + kl_c)^2 \tilde{A}^2 / 4\pi, \quad (36a)$$

$$\tilde{K}_e = k\tilde{A}^2 / 4\pi. \quad (36b)$$

The spectral dependences of the energies and helicities for these waves are shown in Fig. 2 (two-species magnetofluid) and Fig. 3 (MHD). Table II shows their limiting trends for low k ($kl_c < 1$) and high k ($kl_c > 1$). In a two-species magnetofluid [Fig. 2(a)] the magnetofluid energies of the three waves are roughly the same for low k , but the R wave is the energetically favorable (lowest energy) wave for high k . The selection of the R wave (“whistler” for $k > l_c$) as the energetically favorable wave is consistent with results from numerical simulations²⁷ that show the whistler as the active wave in two-fluid reconnection. For low k there is an equipartition between the magnetic and kinetic energies, while at high k , the magnetic energy dominates in the favored wave. Further, the ion helicity is mainly carried by low k modes, since \tilde{K}_i is very small at high k (in the favored wave). In MHD (Fig. 3) the magnetofluid energy is not shown because it is identical to the low- k behavior in Fig. 2 extended to all k . Thus in MHD the energy equipartition holds for all k . The three MHD helicities (magnetic, cross, kinetic) have power-law scalings with k [Eq. (35)]. However, \tilde{K}_i differs from low to high k ; this will prove significant in considering cascades.

The foregoing treatment assumed a nondrifting and cold plasma. Adding drifts introduces a Doppler shift of the frequency and corrections mainly at small wave numbers. Adding “warm” plasma effects introduces a finite sound speed

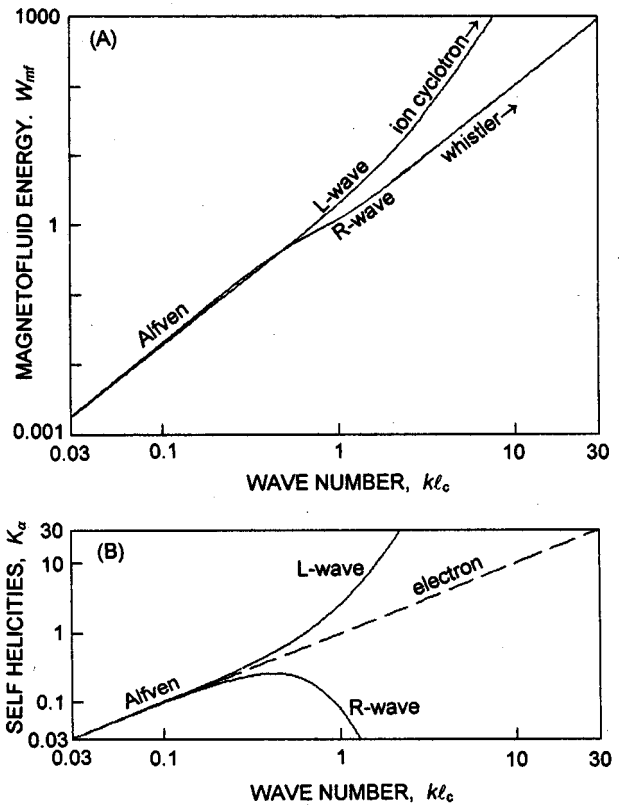


FIG. 2. Wave energy (A) and self-helicities (B) for a two-fluid. The normalizations are $|A|^2/16\pi l_c^2$ (energy) and $|A|^2/4\pi l_c$ (self-helicities).

c_s . Then the phase velocity of the magnetoacoustic wave increases to $\omega/k = (c_s^2 + v_A^2)^{1/2}$, and a new wave (slow wave) appears with phase velocity between c_s and $v_A c_s / (c_s^2 + v_A^2)^{1/2}$, depending on the direction of \mathbf{k} . Since $c_s = (\beta/2)^{1/2} v_A$ (β is the ratio of the pressure to the magnetic pressure) the lower-frequency slow wave has a stronger ion response for $\beta < 1$. In any case, warm plasma effects slightly modify the waves of the cold-plasma approximation and introduce a new wave with similar properties. Having established the fluid-field coupling, we can now test the ruggedness of the global invariants.

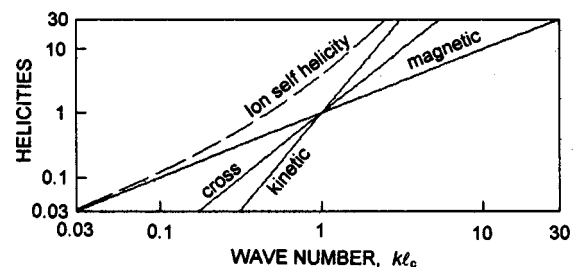


FIG. 3. Helicities in MHD. The normalizations are $|A|^2/4\pi l_c$ (magnetic), $(e/m_i c)|A|^2/l_c^2$ (cross), $(e/m_i c)^2|A|^2/l_c^3$ (kinetic), and $|A|^2/4\pi l_c$ (ion self-helicity).

TABLE II. Limiting behavior of waves.

Two-species fluid	Low $k(kl_c \ll 1)$	High $k(kl_c \gg 1)$
Frequency, energy	$\omega/\omega_{ci}, 8\pi\tilde{W}_{mf}/ \tilde{A} ^2$	$\omega/\omega_{ci}, 8\pi\tilde{W}_{mf}/ \tilde{A} ^2$
R wave (k_{\parallel})	$kl_c, 2k^2$	$(kl_c)^2, k^2[1+(kl_c)^{-6}]$
L wave (k_{\parallel})	$kl_c, 2k^2$	$1-(kl_c)^{-2}, k^4l_c^2$
Energy partition	$\tilde{W}_m \sim 1$	$\tilde{W}_m \sim 1$
($8\pi\tilde{W}/ \tilde{A} ^2$)	$\tilde{W}_f \sim 1$	$\tilde{W}_f \sim 0$
Self-helicities (R wave)	$\tilde{K}_i \sim k$	$\tilde{K}_i \sim 0$
($8\pi\tilde{K}_\alpha/ \tilde{A} ^2$)	$\tilde{K}_e \sim k$	$\tilde{K}_e \sim k$
MHD		
Frequency, energy	$\omega/\omega_{ci}, 8\pi\tilde{W}_{mf}/ \tilde{A} ^2$	$\omega/\omega_{ci}, 8\pi\tilde{W}_{mf}/ \tilde{A} ^2$
Alfvén wave (k_{\parallel})	$kl_c, 2k^2$	same as low k
Helicities ($8\pi\tilde{K}/ \tilde{A} ^2$)		
Magnetic	$\tilde{K}_m = k$	same as low k
Cross	$\tilde{K}_x = k^2(\nu_A/B_0)$	same as low k
Kinetic	$\tilde{K}_k = k^3(\nu_A/B_0)^2$	same as low k
(Ion self)	$\tilde{K}_i \sim k$	$\tilde{K}_i \sim k^3l_c^2$

B. Inverse cascade

An inverse cascade of helicity is its evolution towards small wave numbers leading to the generation of a large-scale magnetofluid object. In a relaxing plasma this is a non-linear process involving two kinds of wave interactions: between waves of different types and between waves of the same type but different k . Whether the evolution is toward larger or smaller scale objects depends on the energy and helicity content of waves. In the previous section we observed that the R-wave has the lowest energy at a given k ; thus this wave type is energetically favored. Here we consider interactions between waves of the same type, applying a theorem based on the spectral properties of the energy and helicity. If they satisfy the inequality

$$\tilde{W}(k) \geq k\tilde{K}(k) \tag{37}$$

then the simultaneous transfer of both energy and helicity to small scales is impossible, and an *inverse* cascade of both helicity and energy is allowed. This was proved using ideal triad wave interactions for two-dimensional Navier–Stokes flows,²⁸ and ideal MHD.²¹ (See also Ref. 1.) In a two-fluid we established the inequality [Eq. (37)] for \tilde{W}_{mf} with both \tilde{K}_i and \tilde{K}_e (Fig. 2, Table II). Therefore both self-helicities pass the inverse cascade test. This argument contradicts a suggestion elsewhere [p. 134 of Ref. 7] that K_i is unlikely to survive because small-scale fluctuations will affect it quite differently from K_e . While the two k dependences differ significantly [Fig. 2(b)], they do so in a way that shows \tilde{K}_i to be even more rugged since it becomes quite small for high k .

Returning to MHD, the Frisch argument assuredly *does not apply* to the cross and kinetic helicities since (see Fig. 3, Table II) they do not satisfy the inequality [Eq. (37)]. For the cross helicity no cascade is anticipated, and for the kinetic helicity a *normal* cascade (toward *higher* k) is anticipated since the inequality is *reversed*. Note, with respect to \tilde{K}_i , the Frisch inequality [Eq. (37)] only applies for *low* k in MHD

[Eq. (36a)]. Thus a two-fluid simulation should exhibit rugged K_i , but an MHD simulation may completely miss this property.

C. Selective decay

The second test of ruggedness is *selective decay*, articulated by Montgomery and associates^{20,22} and Taylor.³ In the presence of weak dissipation, is a particular helicity *more invariant* than the magnetofluid energy? This can be approached either by a spectral argument or by comparison of actual decay rates. The former arises from the inequality analogous to Eq. (37): \tilde{W}_{mf} is proportional to a higher power of k than \tilde{K}_α so that its spectrum should peak at a higher k . Since dissipation is stronger at higher k (smaller scale) the magnetofluid energy should be dissipated faster than either self-helicity. Indeed this tendency is accentuated for \tilde{K}_i because of its smallness at high k .

The second form of the selective decay argument compares the decay rates of the magnetofluid energy and the self-helicities. The evolution of the specific self-helicity is given by Eq. (13). The specific friction force,

$$\frac{\mathbf{R}_\alpha}{n_\alpha} = -q_\alpha \boldsymbol{\eta} \mathbf{j} + \frac{\nabla \cdot \boldsymbol{\Pi}_\alpha}{n_\alpha} \tag{38}$$

includes both resistivity, $\boldsymbol{\eta} = m_e/e^2 n \tau_e$ (τ_e = electron collision time), and the viscous stress tensor, $\boldsymbol{\Pi}_\alpha$. Here we assume a simplified form of the viscous stress, $\nabla \cdot \boldsymbol{\Pi}_\alpha \approx \nu_\alpha \nabla^2 \mathbf{u}_\alpha$, where ν_α is the viscosity coefficient. Multiplying Eq. (13) by $c^2/4\pi q_\alpha^2$ and integrating over the system volume gives the decay of the global self-helicities:

$$\frac{dK_\alpha}{dt} = -\frac{c^2}{4\pi q_\alpha^2} \int d\tau \boldsymbol{\Omega}_\alpha \cdot \left(-q_\alpha \boldsymbol{\eta} \mathbf{j} + \frac{\nu_\alpha}{n} \nabla^2 \mathbf{u}_\alpha \right). \tag{39}$$

The decay of the magnetofluid energy includes resistive and viscous dissipation terms:

$$\frac{dW_{mf}}{dt} = \int d\tau \left(\eta j^2 + \sum_{\alpha} \nu_{\alpha} |\nabla u_{\alpha}|^2 \right). \quad (40)$$

Hereafter we neglect the electron viscosity since it is smaller by the mass ratio. The ion viscosity is related to the resistivity in a simple way,

$$\nu_i = \mu_{\tau} m_i n \beta_i \eta c^2 / 8\pi, \quad (41)$$

where $\beta_i = 8\pi n k T_i / B^2$ and $\mu_{\tau} \equiv m_i \tau_e / m_e \tau_i$ is a modified mass ratio: for $T_i = T_e$, $\mu_{\tau} = (m_i / 2m_e)^{1/2} \approx 40$ for deuterons. For shear viscosity, the form $\nu_i \nabla^2 \mathbf{u}_i$ only holds for $\nabla < 1/\rho_i$ where $\rho_i = c(m_i k T_i)^{1/2} / eB = l_c (\beta_i / 2)^{1/2}$ is the ion gyroradius; therefore the shear stress has the approximate upper bound, $|\nu_{i\perp} \nabla \mathbf{u}_i| \leq \nu_{i\perp} |u_i| / \rho_i$. Similarly for the parallel viscosity, the form $\nu_i \nabla^2 \mathbf{u}_i$ only holds for $\nabla < 1/\lambda_i$, where $\lambda_i = (k T_i / m_i)^{1/2} \tau_i$ is the ion mean free path; therefore the parallel viscosity has the upper bound, $|\nu_{i\parallel} \nabla u_i| \leq \nu_{i\parallel} |u_i| / \lambda_i$. Note that accounting for the anisotropy of the ion viscosity coefficient, the two upper bounds are the same: $\nu_{i\perp} |u_i| / \rho_i \approx \nu_{i\parallel} |u_i| / \lambda_i$.

Now consider large k ($kl_c > 1$) reflecting the range where significant dissipation is expected. The limits $k > 1/l_c$ and $k > 1/\rho_i$ are roughly equivalent, so that the upper bound on the viscous stress applies. Further, we use the perturbed magnetic field in the singular layer, $\tilde{\mathbf{B}} = i\mathbf{k} \times \tilde{\mathbf{A}}$, as the primary field quantity. Then the rates of change are

$$dK_e / dt \sim k \frac{\eta c^2}{4\pi} \frac{|\tilde{\mathbf{B}}|^2}{8\pi}, \quad (42)$$

$$dK_i / dt \sim k \frac{\eta c^2}{4\pi} \frac{|\tilde{\mathbf{B}}|^2}{8\pi} \left[2 + \frac{\mu_{\tau}}{k^2 l_c^2} \right], \quad (43)$$

$$dW_{mf} / dt \sim k^2 \frac{\eta c^2}{4\pi} \frac{|\tilde{\mathbf{B}}|^2}{8\pi} \left[1 + \frac{\mu_{\tau}}{k^2 l_c^2} \right]. \quad (44)$$

The μ_{τ} terms represents the viscosity, while the other term is the resistivity. Although $\mu_{\tau} \approx 40$, it is clear that the predominant decay scalings are $dK_{\alpha} / dt \propto k$, and $dW_{mf} / dt \propto k^2$. These are the same proportionalities observed by Taylor³ in comparing the decays of K_m and W_m . Thus the energy will be dissipated more strongly than either self-helicity in thin reconnection layers, i.e., the self-helicities are ‘‘rugged.’’

In the foregoing selective decay argument note the importance of two factors that apply in singular layers: (1) the viscous force is bounded $\sim \nu_{i\perp} |u_i| / \rho_i$ rather than the much larger ‘‘standard formula’’ $\nu_{i\perp} |u_i| k$; and (2) the ion velocity takes the *high-k* behavior $\tilde{u}_i \sim k^{-1} (e\tilde{B} / m_i c)$, rather than the MHD-like $\tilde{u}_i \sim l_c (e\tilde{B} / m_i c)$. If these two factors were ignored [p. 134 of Ref. 7], then the decays proportionalities would be $dK_i / dt \propto k^3$, and $dW_{mf} / dt \propto k^2$. Then selective decay would preferentially dissipate the ion helicity, just as it preferentially dissipates the kinetic helicity in a pure fluid.¹⁰

D. Stability to resistive modes

Arguments for the ruggedness of the magnetic helicity based on relative time scales has been advanced by Park *et al.*²³ and more recently by Edenstrasser and Kassab.²⁹ Park addressed the decay of magnetic helicity that occurs in

relatively thin reconnection layers, which occupy a small fraction of the system volume. Topology changes (reconnections) are ‘‘rapid’’ if they occur at the rate $d\psi_s / dt \sim \eta^{\sigma}$ with $\sigma < 1$ (ψ_s is the magnetic flux at the x point of the singular layer). Both the Sweet–Parker ($\sigma = 1/2$) and Petschek ($\sigma = 0$) scalings represent ‘‘rapid’’ reconnection. If the change in an invariant has the scaling $dK / dt \propto \eta$, then it is ‘‘stable’’ to resistive modes, i.e., it is invariant on the time scale of the topology change. This holds for the magnetic helicity, K_m , as follows

$$\frac{dK_m}{dt} = \int d\tau \eta \mathbf{j} \cdot \mathbf{B} \sim \eta \int_{\delta} dx j \sim \eta, \quad (45)$$

where x is the coordinate across the thin singular layer of thickness δ . The same argument can be extended to the self-helicities, in particular the ion self-helicity, for which the rate of change [from Eq. (39)] is

$$\frac{dK_i}{dt} = \frac{c^2}{4\pi e} \int d\tau \left(\eta \mathbf{j} - \frac{\nu_i \nabla^2 \mathbf{u}_i}{en} \right) \cdot \left[\mathbf{B} + \nabla \times \left(\frac{m_i c \mathbf{u}_i}{e} \right) \right], \quad (46)$$

where ν_i is the viscosity. Consider the additional terms appearing in the two factors of Eq. (46) compared with Eq. (45). In the first factor $\eta \mathbf{j}$ is augmented by the viscous term $(\nu_i / en) \nabla^2 \mathbf{u}_i$, the magnitude of which can be estimated. Express $\nu_i / n \approx m_i^{3/2} m_e^{-1/2} \beta_i \eta c^2 / 8\pi$; introduce the bound on the viscous stress $|\nabla^2 \mathbf{u}_i| < |u_i| / \rho_i^2$; and employ the high- k ion response $\mathbf{u}_i \approx -e\mathbf{A} / m_i c$. Further, $4\pi \mathbf{j} / c = i\mathbf{k}_R \times \mathbf{B} \sim k_R^2 \mathbf{A}$, so that $\mathbf{A} \sim 4\pi \mathbf{j} / ck_R^2$ (here k_R is the inverse length scale associated with the reconnection layer thickness). Finally with the identity, $\beta_i / 2\rho_i^2 = 1/l_c^2$, these expressions combine to simplify the viscous stress term: $|(\nu_i / en) \nabla^2 \mathbf{u}_i| < (m_i / m_e)^{1/2} (k_R l_c)^{-2} \eta |\mathbf{j}|$. For thin singular layers (specifically, $k_R l_c > (m_i / m_e)^{1/4} \sim 8$) the viscous stress term is comparable to or less than the basic term $\eta \mathbf{j}$. In the square-brackets factor of Eq. (46): \mathbf{B} is augmented by a vorticity term $\nabla \times (m_i c \mathbf{u}_i / e)$. With $\mathbf{u}_i \approx -e\mathbf{A} / m_i c$ as before, this is $\nabla \times (m_i c \mathbf{u}_i / e) \approx \nabla \times \mathbf{A} \approx \mathbf{B}$, i.e., it is comparable to the basic term. Concluding that since the additional terms in the ion self-helicity are comparable to the terms appearing in the magnetic helicity, it follows [from Eq. (45)] that $dK_i / dt \sim \eta$ also. Thus the ion self-helicity should also be stable to resistive modes.

IV. EQUATIONS OF RELAXED-STATE EQUILIBRIA

A. Minimization principal: Euler equations

The theory of relaxation postulates that a weakly dissipative system approaches the maximal-entropy state of the ideal (nondissipative) system.^{16,20} An essential element of such theories is the adoption of constraints. We have already discussed invariant helicities at length. Beside these, a closed system also has invariant total energy, mass, and a global momentum invariant (supposing a symmetric boundary). An alternative approach to finding relaxed states is energy minimization. This minimizes the organized energy form, i.e., the magnetofluid energy W_{mf} rather than the total energy (which

is conserved in a closed system). These two approaches are compared and found partially interchangeable.

The maximal entropy state is found by the variational principle,^{8,15,16}

$$\delta S - \eta \delta W - \mu \delta M - V_q \delta L_q - \lambda_i \delta K_i - \lambda_e \delta K_e = 0. \quad (47)$$

Here $S = \int d\tau n \ln(p/n^\gamma)$ is the entropy (where p is the sum of ion and electron pressures); η , μ , V_q , λ_i , and λ_e are Lagrange multipliers associated with the total energy, $W = W_{mf} + \int d\tau p/(\gamma - 1)$; mass, $M = \int d\tau \sum m_\alpha n_\alpha$; global momentum, $L_q = \int d\tau \sum m_\alpha n_\alpha \mathbf{u}_\alpha \cdot \mathbf{q}$; and self-helicities, respectively. Observe that the total energy is the sum of the organized (magnetic+flow) and disorganized (thermal) forms. The vector \mathbf{q} in the momentum depends on the symmetry: for an axisymmetric boundary (conserved angular momentum), $\mathbf{q} = r\hat{\theta}$; and for a ‘‘cylindrical’’ boundary with an ignorable coordinate (z), $\mathbf{q} = \hat{z}$. The minimum energy state is found by the variational principle,^{2,6,9,14}

$$\delta W_{mf} - V'_q \delta L_q - \lambda'_i \delta K_i - \lambda'_e \delta K_e = 0, \quad (48)$$

where V'_q , λ'_i , λ'_e are the Lagrange multipliers associated with the global momentum, and self-helicities, respectively.

Evidently adding constraints modifies the resulting relaxed state; further, two invariant helicities foster *two* corresponding Euler equations.⁶ In terms of variations of the flow and field variables ($\mathbf{u}_i, \mathbf{u}_e, \mathbf{A}$) the entropy and energy principles are equivalent. Taking independent variations, $\delta \mathbf{u}_\alpha$ ($\alpha = i, e$) gives

$$(\mathbf{u}_\alpha - V'_q \mathbf{q}) = 2\lambda'_\alpha (l'_c/m_i) \mathbf{\Omega}_\alpha. \quad (49)$$

These are consistent with Euler equations found elsewhere⁶⁻⁹ although they account for features missing in earlier derivations: electron inertia;^{6,7} nonuniform ambient density;⁶ recognition of *both* self-helicities;⁹ and conserved angular momentum.⁶⁻⁹ An advantage of the form in Eq. (49) is the symmetric treatment of each species and the recognition of the natural length scale $l_c = c/\omega_{pi}$. Thus in a relaxed state the flow velocity of each species is proportional to its generalized vorticity: the velocity is shifted by the angular momentum constraint, and the Lagrange multiplier (constant of proportionality) plays a role like an eigenvalue. Taking the independent variation, $\delta \mathbf{A}$, gives

$$\nabla \times \mathbf{B} = (c/e)(2\lambda'_i \mathbf{\Omega}_i - 2\lambda'_e \mathbf{\Omega}_e). \quad (50)$$

If the $2\lambda'_\alpha \mathbf{\Omega}_\alpha$ are eliminated using Eq. (49) then this reduces to the steady form of Ampere’s law. These three equations [Eq. (49) with $\alpha = i, e$, and Eq. (50)] are equivalent to results from the same three variations applied to the entropy minimization principle, and the Lagrange multipliers are related by $\lambda'_\alpha = -\lambda_\alpha/\eta$ and $V'_q = -V_q/\eta$.

In the reduced case of MHD there is no ion helicity invariant. This invariant can be dropped in the foregoing formulation simply by setting the associated multiplier, λ_i , to zero. Consequently Eq. (49) with $\alpha = i$ becomes $\mathbf{u}_i = V'_q \mathbf{q}$. Recognizing $\mathbf{j} = en(\mathbf{u}_i - \mathbf{u}_e)$ and $\nabla \times \mathbf{q} = 0$, Eq. (49) with $\alpha = e$ then becomes $2\lambda'_e \mathbf{B} = (4\pi/c)\mathbf{j}$. This is the familiar equation for a force-free state, which is the relaxed state in MHD.

B. Bernoulli equation

The presence of invariants linking the field and fluid elements allows the existence of finite pressure in the relaxed state^{9,15,16} and was demonstrated for the ion helicity by Turner.⁶ The pressure is found using the steady equation of motion, $\sum m_\alpha n_\alpha \mathbf{u}_\alpha \cdot \nabla \mathbf{u}_\alpha = \nabla p + \sum (q_\alpha n_\alpha \mathbf{u}_\alpha / c) \times \mathbf{B}$. This can be placed in an equivalent containing the generalized vorticity by expanding $\mathbf{u}_\alpha \cdot \nabla \mathbf{u}_\alpha$ and recognizing that $\mathbf{B} = \nabla \times \mathbf{A}$:

$$\nabla p/n + \nabla \left(\sum_\alpha m_\alpha u_\alpha^2 / 2 \right) = \sum_\alpha \mathbf{u}_\alpha \times \mathbf{\Omega}_\alpha. \quad (51)$$

For a relaxed state this simplifies further: expand $\mathbf{u}_i \cdot \nabla \mathbf{u}_i$ using a vector identity and replace $\mathbf{j} = en(\mathbf{u}_i - \mathbf{u}_e)$ from Eq. (49). Then assuming massless electrons

$$\frac{\nabla p}{m_i n} + \nabla \left(\frac{u_i^2}{2} \right) + \frac{V'_q}{2l_c^2} \sum_\alpha \frac{\mathbf{u}_\alpha \times \mathbf{q}}{\lambda'_\alpha} = 0. \quad (52)$$

This is a Bernoulli equation in that it relates the pressure to the flow velocity without reference to the magnetic field.^{12,15} Then pressure gradients are maintained only by the Bernoulli effect, and the only coupling to the magnetic field is through the flow velocity. Further, Eq. (52) is an exact derivative and can be integrated as follows. For a barotropic plasma [$p = p(n)$, see Eq. (6)] with $h_\alpha = \int dp_\alpha/n$, the first term is $\nabla h_\alpha/m_i$. The third term can be simplified by recognizing that stream functions, ψ_α , must exist because of continuity. For axisymmetry ($\mathbf{q} = r\hat{\theta}$), $n\mathbf{u}_\alpha = nu_{\alpha\theta}\hat{\theta} + \nabla\psi_\alpha \times \hat{\theta}/r$, where $u_{\alpha\theta}$, $\psi_\alpha = f(r, z)$; then the third term becomes $-\nabla[(V'_q/2nl_c^2)\sum\psi_\alpha/\lambda'_\alpha]$, while for linear symmetry ($\mathbf{q} = \hat{z}$), $n\mathbf{u}_\alpha = nu_{\alpha z}\hat{z} + \nabla\psi_\alpha \times \hat{z}$, where $u_{\alpha z}$, $\psi_\alpha = f(x, y)$; and the third term is the same except V'_z replaces V'_θ . Here we recognized $nl_c^2 = \text{const}$. Then Eq. (52) can be integrated:

$$\sum_\alpha h_\alpha + m_i u_i^2 / 2 - V'_q (2\pi e^2 / c^2) \sum_\alpha \psi_\alpha / \lambda'_\alpha = \text{const}. \quad (53)$$

This form of the Bernoulli equation differs from its pure-fluid counterpart in that it is global, i.e., the *constant* is global rather than a function of the particular streamline. Equation (53) suggests that finite β needs only a gradient of u_i^2 rather than the more restrictive requirement of nonzero generalized vorticity.⁶

Although the pressure is related to the velocity alone, this does not imply force-free states as observed elsewhere.¹⁵ This is easily seen for an isothermal plasma, $h_\alpha = kT_\alpha \ln p_\alpha$, with no global momentum constraint. Then $p_\alpha = \text{const} \times \exp(-m_i u_i^2 / 2kT_\alpha)$ so that the pressure *falls* toward the plasma edge if the flow speed rises toward the edge. This is the opposite of force-free MHD where (e.g., for rigid rotation) centrifugal forces cause the pressure to *rise* toward the edge.

V. EXAMPLE RELAXED EQUILIBRIA

A. Classification of relaxed states

The appeal of a relaxation theory is that the ‘‘relaxed’’ state can be found given certain initial parameters alone, i.e., the theory has predictive power. In this, the more general

TABLE III. Specifications that classify relaxed states.

Class of equilibrium	K_i	K_e	boundary condition
	(reference to aW_B)		
Toroids			
Tokamak	small	small	specify ψ_{toroidal}
RFP	0	moderate	specify ψ_{toroidal}
Compact toroids			
Spheromak	0	moderate	$B_{\text{toroidal}}=0$
FRC	0	0	$B_{\text{toroidal}}=0$

multifluid theory is not fundamentally different from the MHD theory, only more complex by having a multiple (M, W, L_θ, K_i, K_e) rather than a single (K_m) constraint. Consequently, the variety of relaxed equilibria for a two-fluid is much broader than for MHD. Each added constraint (e.g., K_i) carries with it one new parameter, its Lagrange multiplier (e.g., λ_i). Relaxed states with invariant self-helicities have been examined elsewhere^{6,8,9} including an approach that expresses the solution in terms of eigenvectors.⁶ Here, for the sake of example, we focus attention on two particular kinds of equilibria, FRCs and tokamaks.

The class of relaxed equilibrium depends on two types of conditions: the values of invariants and the boundary conditions. These vary from one configuration to another as illustrated in Table III. Here the size of the self-helicities are referenced to the product aW_B where a is the nominal system dimension (minor radius) and W_B is the magnetic energy. The four classes represent “pure” equilibria. Not shown are intermediate states, e.g., between FRC and spheromak. Also not shown are other invariants (M, W, L_θ) which are less important in determining the class of equilibrium. Force-free equilibria (RFP, spheromak) are included in the range of relaxed states (Table III) but are well known and not presented here. For simplicity we adopt simplified one-dimensional geometries. The one-dimensional analogies used here are the sheet pinch and the straight z pinch. The general equations governing relaxed states are Eqs. (49), (50), (53), and the barotropic equation $p=p(n)$. In addition to the invariants and boundary conditions (Table III) there are regularity conditions, i.e., the poloidal magnetic field and flow speeds (or their geometric analogies) must vanish at the magnetic axis.

B. FRC relaxed state

FRCs are typically an elongated compact toroid; therefore we adopt the sheet pinch analogy. Imagine that the magnetic surfaces are elongated infinitely, stretching the magnetic axis into a neutral sheet; then “cut” the azimuthal coordinate and unwind it to straighten out the neutral sheet into a flat plane. This produces a slab equilibrium with one nonignorable coordinate. In Cartesian coordinates x, y, z are analogous to the minor radius (nonignorable), toroidal, and poloidal coordinates, respectively, and $x=0$ (neutral sheet) represents the magnetic axis. Since a strictly one-dimensional geometry has no magnetic separatrix, the definition of the separatrix is arbitrary. We identify the separatrix as the system boundary. Size scales in the analogous cylin-

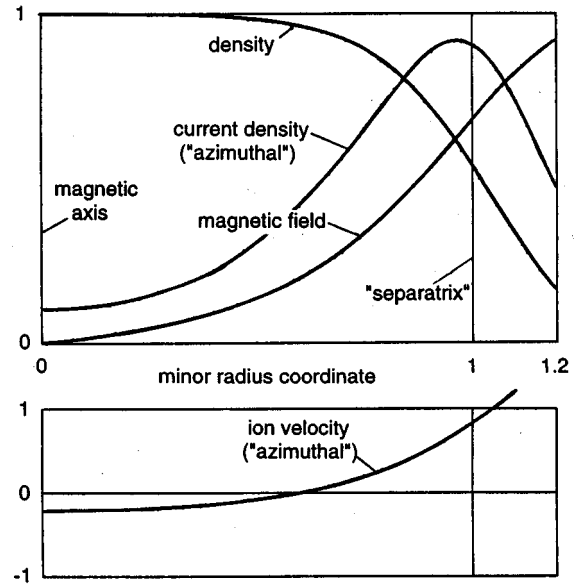


FIG. 4. Example of a relaxed-state FRC in a slab equilibrium. Other properties of this example: $V'_z=0.30(kT/m_i)^{1/2}$ (consistent with $L_z=0$); $\lambda_i \rightarrow \infty$ (consistent with $K_i=0$); $\lambda_e=0.0008/l_{c0}$ (consistent with $K_e=0$); separatrix density, $n_s/n_0=0.54$; ion flow speed at magnetic axis, $u_z(0)=0.23(kT/m_i)^{1/2}$; minor radius parameter, $s=\int r dr/r_s \rho_i=1.04$ (integral over the minor radius); and current profile index, $h=j_y(x=0)/\langle j_y \rangle=0.26$.

dricl coordinate geometry are related to the sheet-pinch minor radius as follows: major radius, $R=2a$; separatrix radius, $r_s=\sqrt{8}a$; and minor radius coordinate, $x=r^2/R^2-1$. The external magnetic field satisfies $n_0kT=B_{\text{ext}}^2/8\pi$.

We have computed a representative relaxed FRC equilibrium with the following assumptions. (a) It is a “pure” FRC: $K_i=K_e=0$. Further, it has no net global momentum, $L_z=0$; this assumption is insignificant in the sheet pinch which has no centrifugal effect. (b) The average β inside the separatrix is determined by the average- β condition, as if the configuration had finite length: in a straight coil this condition relates $\langle \beta \rangle$ to the ratio of the separatrix to the magnetic coil radius.³⁰ Here $\langle \beta \rangle=0.92$ is chosen, which corresponds to a typical separatrix to coil radius ratio of 0.4. (c) The mass inventory was chosen so as to give the radius parameter, $S_* = r_s/l_{c0}=10$ (r_s =separatrix radius, l_{c0} corresponds to n_0). (d) Uniform temperature is assumed. The structure of this relaxed-state FRC is shown in Fig. 4. Here the relaxed state was extended outside the separatrix (system boundary). This example resembles laboratory FRCs in several respects: (1) high β , with a nearly magnetic field-free core; (2) longitudinal-magnetic field only; (3) hollow current profile, i.e., current density minimum at the magnetic axis;³¹ (4) significant rotational flow speeds; and (5) a natural plasma edge with length scale comparable to l_c , which is somewhat smaller than the plasma size. This edge arises naturally without invoking outflow beyond the separatrix.

Although the example in Fig. 4 resembles laboratory FRCs, there is a hidden size-scale difference between the two-fluid model and a more realistic model accounting for finite ion orbit size. This is obscured in the case of FRCs

(which have $\beta \sim 1$) because the ion gyroradius is comparable to the natural length scale, l_c . In an FRC then, the two-fluid model should predict equilibria with length scales that differ from that of a finite-gyroradius plasma only by factors of order unity. This factor may be as much as 2–4 based on a comparison of marginal stability conditions in a two-fluid and gyrofluid.³² This discrepancy is somewhat larger in tokamaks, as will be seen shortly. A further limitation of this simple example is the absence of field line curvature and toroidal effects. The interplay of adverse field line curvature (an inescapable feature of FRCs) and the compensating effect of flow shear in a relaxed state calls for investigation.

C. Tokamak relaxed state

Tokamaks are stabilized against fast ideal modes by a strong toroidal magnetic field, disabling the fast channel for relaxation. Even so a tokamak with a nonrelaxed equilibrium is not a minimum energy state; it therefore has excess energy available to drive a slower relaxation instability. Although the plasma will attempt to relax toward the minimum energy state, powerful profile modifying influences (inductive current drive, neutral beams, radio-frequency current drive) are likely to dominate. In the end, the relaxation tendency may take the form of a microinstability that drives anomalously rapid transport. Therefore even though relaxed states might not appear spontaneously in a tokamak, it is instructive to examine what they would look like.

For a roughly circular cross-section tokamak we adopt the *straight z-pinch* analogy. Imagine here that the toroid is “cut” at a particular toroidal angle, and unwound to make a straight magnetic axis with circular magnetic surfaces. This produces a cylindrical equilibrium with one nonignorable coordinate. In cylindrical coordinates, r, θ, z are analogous to the minor radius (the nonignorable), poloidal, and toroidal coordinates, respectively, and $r=0$ is the magnetic axis. Again, since a strictly one-dimensional geometry has no magnetic separatrix, the definition of the separatrix (minor radius) is arbitrary. The length of the magnetic axis in the toroidal geometry then translates to Aa , where A is the aspect ratio and a is the minor radius. An example relaxed state is shown in Fig. 5 (Ref. 33). Again the boundary is marked by a fiducial and the Euler equations were integrated beyond the system boundary. Observe the following features: (1) reversed magnetic shear (qA profile); (2) hollow current profile; and (3) high flow speed. While the parameters chosen for Fig. 5 (see caption) are somewhat artificial, a broad range of calculations shows that reversed magnetic shear and hollow current profile are natural features of tokamak-like relaxed states.

The example in Fig. 5 resembles the reverse-shear core recently created in two tokamaks.^{34,35} (In the example, the system boundary is analogous to the boundary of the reverse shear region.) The most striking feature of these tokamaks is the spectacular reduction in transport rate in the reversed-shear core. That the core may be in a relaxed state is an intriguing possible explanation: in a relaxed state, the free energy that drives microinstabilities and the attendant anomalous transport is simply absent. Therefore the transport

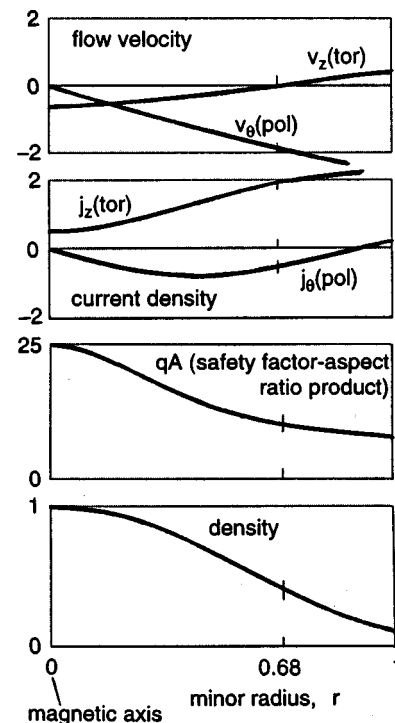


FIG. 5. Tokamak relaxed states. The reference scales are as in Fig. 4. The specifications at the magnetic axis are $\beta_0 = p_0/B^2/8\pi = 0.10$, $q_0A = 25$ (q_0 is the safety factor at the magnetic axis, see Ref. 33), $u_{z0} = 0.6[kT/m_i]^{1/2}$; and at the boundary ($r=a$), $u_z=0$, $p/p_0=0.4$. Other specifications: $qA = 25$ (magnetic axis), 10 (system boundary); $u_{iz} = 0.6(kT)^{1/2}$ (magnetic axis), 0 (boundary); current density profile with an axis/boundary ratio $\approx 1/4$.

may simply revert to classical (or neoclassical).

As mentioned in discussing the FRC example, there is an ignored length scale in the simple two-fluid model, namely the ion orbit size. This was not so important in the case of an FRC because of $\beta \sim 1$. However, in a *low- β* plasma the orbit size is set by the smaller (poloidal) field and can be much larger. In Fig. 5 the boundary radius is $\approx 0.7l_{c0}$, corresponding to 2–4 cm at the observed densities.^{34,35} The length scale correction is the ratio of the toroidal-to-poloidal magnetic fields (orbit size over gyroradius), which is ≈ 10 in Fig. 5, then the boundary radius increases to 20–40 cm; this corresponds roughly with the observed 15–30 cm radii of the reversed-shear core. The incorrect length scale may also be responsible for the unrealistically large poloidal flows found in this example.

VI. DISCUSSION

We have presented a relaxation theory based on a two-fluid model. This treatment encompasses a much broader range of relaxed states than the familiar theory based on the reduced case of MHD. In particular, it allows finite pressure, and predicts significantly sheared flows. Several issues need further examination to place the two-fluid theory on a firmer footing. These are discussed here.

A. Relaxation physics

Extensive studies of the physics of relaxation have been done using the MHD model, including recently, both

analytical³⁶ and numerical³⁷ approaches. However, one of the conclusions of our work is that the single-fluid paradigm fails to capture the invariance of the ion self-helicity, which is essential for the appearance of finite pressure and sheared flows. Evidently two-fluid analyses and simulations are needed. While some two-fluid simulations have been made, these have not specifically addressed relaxation. Notably though, a recent two-fluid simulation of reconnection²⁷ displayed an important feature predicted in our two-fluid theory, namely that the whistler is the active wave in the high- k spectral range. The understanding of the relaxation would also be facilitated by extending the MHD approaches^{20,21} to a two fluid.

B. Stability

Certainly there is the *expectation* that two-fluid relaxed states will have improved stability, and the hope that ideal modes, at least, should be stabilized. If the pressure falls (toward the edge) as the flow velocity increases, this may stabilize ballooning modes,³⁸ and the improvement is most pronounced for configurations with closed magnetic field lines.³⁹ Sheared flow was shown to have a strong stabilizing effect on global modes in a z pinch.⁴⁰ An experiment to test this is presently being constructed by Shumlak and associates at the University of Washington. These expectations need to be placed on a firmer basis, as has been done in the reduced (MHD) model. There, a theorem (for nonflowing MHD) has been found stating that maximal entropy assures stability to all ideal modes.¹⁶ Also, a proof of the stability of force-free states has been given.⁴¹ A similar theorem is needed that links stability to relaxed states of a two-fluid.

C. Comparison with experiment

The spectacular prediction of RFP evolution and structure was what catapulted the MHD relaxation theory into prominence.^{2,3} Similar achievements would advance the two-fluid theory. This might include the following steps. (1) Find a correlation between the predicted profiles in FRCs and experimental observations: this is analogous to the observation of force-free profiles in RFPs and spheromaks. (2) Show that a relaxation that preserves the self-helicities correlates with anomalous magnetic flux dissipation observed in FRC startup;⁴² this is analogous to the observation of magnetic helicity conservation in the startup relaxation of RFPs and spheromaks. (3) Verify the spontaneous appearance of counterflow in FRC startup as predicted by the two-fluid theory; this would be analogous to the appearance of spontaneous field reversal in RFPs.

D. Finite orbit effects

A barrier to quantitative confirmation between theory and experiment is an effect that is ignored in the two-fluid theory, the natural length scale of which is the collisionless skin depth l_c . A more realistic model would account for finite ion orbits, and may increase the length scale accordingly. For $\beta \sim 1$ (comparable plasma and magnetic pressures) as in an FRC, the ion gyroradius is comparable to l_c so

that size differences are of order unity. The discrepancy is even larger in a tokamak where the orbit size is based on the smaller of the two field components. Evidently, the two-fluid theory needs to be extended to include finite orbit effects. One approach might be to develop a relaxation theory based on a gyroviscous two-fluid. Such a theory is necessary for a quantitative experimental confirmation of the theory.

E. Effect on transport

Both resistivity and viscosity play a role in dissipation. Both will drive a plasma away from a relaxed state and set off a ‘‘correction’’ in the form of a relaxation that restores the relaxed state. This synthesis of dissipative and relaxation processes may be a critical ingredient in understanding the anomalous transport in tokamaks and FRCs and needs critical examination.

ACKNOWLEDGMENTS

The authors thank R. N. Sudan who suggested to us the self-helicities as invariants, and also M. R. Brown, W. Park, M. J. Schaffer, and the referee for helpful comments.

APPENDIX: CONVECTION OF GENERALIZED VORTEX LINES WITH THE FLUID

We prove here that generalized vortex lines convect with the particular species. Suppose we choose a line that initially is everywhere tangential to the local generalized vortex, i.e., $\mathbf{\Omega}_\alpha \times d\mathbf{x} = 0$ at $t=0$, where $d\mathbf{x}$ an increment of that line. Suppose further that at time advances, that line convects with species α . The evolution of the quantity $\mathbf{\Omega}_\alpha \times d\mathbf{x}$ on the moving line is determined by the total derivative, $D_\alpha(\mathbf{\Omega}_\alpha \times d\mathbf{x})/Dt$. Expand this; use Eq. (9); eliminate the density using continuity, $D_\alpha n_\alpha/Dt = -n_\alpha(\nabla \cdot \mathbf{u}_\alpha)$; and use the kinematic relation $D_\alpha(d\mathbf{x})/Dt = d\mathbf{x} \cdot \nabla \mathbf{u}_\alpha$. Then

$$D_\alpha(\mathbf{\Omega}_\alpha \times d\mathbf{x})/Dt = -(\nabla \cdot \mathbf{u}_\alpha)\mathbf{\Omega}_\alpha \times d\mathbf{x} - d\mathbf{x} \times (\mathbf{\Omega}_\alpha \cdot \nabla \mathbf{u}_\alpha) + \mathbf{\Omega}_\alpha \times (d\mathbf{x} \cdot \nabla \mathbf{u}_\alpha). \quad (\text{A1})$$

Apply the obscure but easily verified identity,

$$\mathbf{A} \times (\mathbf{B} \cdot \nabla \mathbf{C}) - \mathbf{B} \times (\mathbf{A} \cdot \nabla \mathbf{C}) = -\nabla \mathbf{C} \cdot (\mathbf{A} \times \mathbf{B}) + (\mathbf{A} \times \mathbf{B}) \cdot \nabla \mathbf{C} \quad (\text{A2})$$

to the second and third terms on the right side of Eq. (A1); one of the resulting terms cancels the first term on the right side of Eq. (A1). This leaves

$$D_\alpha(\mathbf{\Omega}_\alpha \times d\mathbf{x})/Dt = -\nabla \mathbf{u}_\alpha \cdot (\mathbf{\Omega}_\alpha \times d\mathbf{x}). \quad (\text{A3})$$

Therefore if the quantity $\mathbf{\Omega}_\alpha \times d\mathbf{x}$ is initially zero on the line composed of increments $d\mathbf{x}$, then as that line convects (with species α), $\mathbf{\Omega}_\alpha \times d\mathbf{x}$ will remain zero. Thus the generalized vorticity remains tangential to that line as it convects with species α , i.e., generalized vortex lines convect with the species.

¹M. R. Brown, J. Plasma Phys. **52**, 203 (1997).

²J. B. Taylor, Phys. Rev. Lett. **33**, 1139 (1974).

³J. B. Taylor, Rev. Mod. Phys. **58**, 741 (1986).

⁴L. C. Steinhauer and A. Ishida, Phys. Rev. Lett. **79**, 3423 (1997).

- ⁵D. K. Bhadra and C. Chu, *J. Plasma Phys.* **33**, 257 (1985).
- ⁶L. Turner, *IEEE Trans. Plasma Sci.* **14**, 849 (1986).
- ⁷K. Avinash and J. B. Taylor, *Comments Plasma Phys. Control. Fusion* **14**, 127 (1991).
- ⁸K. Avinash, *Phys. Fluids B* **4**, 3856 (1992).
- ⁹S. R. Oliveira and T. Tajima, *Phys. Rev. E* **52**, 4287 (1995).
- ¹⁰H. K. Moffatt, *J. Fluid Mech.* **35**, 117 (1969).
- ¹¹L. Woltjer, *Proc. Natl. Acad. Sci. USA* **44**, 833 (1958).
- ¹²R. N. Sudan, *Phys. Rev. Lett.* **42**, 1277 (1979).
- ¹³W. M. Elsasser, *Rev. Mod. Phys.* **28**, 135 (1956).
- ¹⁴L. Woltjer, *Proc. Natl. Acad. Sci. USA* **44**, 489 (1958).
- ¹⁵J. M. Finn and T. M. Antonsen, Jr., *Phys. Fluids* **26**, 3540 (1983).
- ¹⁶E. Hameiri and J. H. Hammer, *Phys. Fluids* **25**, 1855 (1982).
- ¹⁷T. H. Jensen and M. S. Chu, *Phys. Fluids* **27**, 2881 (1984).
- ¹⁸M. A. Berger and G. B. Field, *J. Fluid Mech.* **147**, 133 (1984).
- ¹⁹B. N. Kuvshinov and T. J. Schep, *Phys. Plasmas* **4**, 537 (1997).
- ²⁰D. Montgomery, L. Turner, and G. Vahala, *Phys. Fluids* **21**, 757 (1978).
- ²¹U. Frisch, A. Pouquet, J. Leorat, and A. Mazure, *J. Fluid Mech.* **68**, 769 (1975).
- ²²W. H. Matthaeus and D. Montgomery, *Ann. (N.Y.) Acad. Sci.* **357**, 203 (1980).
- ²³W. Park, D. A. Monticello, and R. B. White, *Phys. Fluids* **27**, 137 (1984).
- ²⁴M. H. Lighthill, *Philos. Trans. R. Soc. London A* **252**, 397 (1960).
- ²⁵R. H. Kraichnan, *J. Fluid Mech.* **59**, 745 (1973).
- ²⁶L. D. Landau and E. M. Lifshitz, *Electrodynamics of Continuous Media* (Pergamon, London, 1959), p. 272.
- ²⁷D. Biscamp, E. Schwarz, and J. F. Drake, *Phys. Plasmas* **4**, 1002 (1997).
- ²⁸R. Fjortoft, *Tellus* **5**, 225 (1953).
- ²⁹J. W. Edenstrasser, *Phys. Plasmas* **2**, 1192 (1995); J. W. Edenstrasser and M. M. M. Kassab, *ibid.* **2**, 1206 (1995).
- ³⁰See Appendix A of W. T. Armstrong, R. K. Linford, J. Lipson, D. A. Platts, and E. G. Sherwood, *Phys. Fluids* **24**, 2068 (1981).
- ³¹L. C. Steinhauer and A. Ishida, *Phys. Fluids B* **4**, 645 (1992).
- ³²A. Ishida, R. Kanno, and L. C. Steinhauer, *Phys. Fluids B* **4**, 1280 (1992).
- ³³In the z -pinch analogy $qA = 2\pi r B_z / L_z B_\theta$ where the pinch length, L_z , is analogous to 2π times the magnetic axis length in toroidal geometry. By analogy, $L_z = 2\pi A r_s$, where A is the aspect ratio and r_s is the minor radius of the boundary; thus $qA = r B_z(r) / r_s B_\theta(r)$.
- ³⁴F. M. Levinton, M. C. Zarnstorff, S. H. Batha, M. Bell, R. E. Bell, R. V. Budny, C. Bush, Z. Chang, E. Fredrickson, A. Janos, J. Manickam, A. Ramsey, S. A. Sabbagh, G. L. Schmidt, E. J. Synakowski, and G. Taylor, *Phys. Rev. Lett.* **75**, 4417 (1995).
- ³⁵E. J. Strait, L. L. Lao, M. E. Mauel, B. W. Rice, T. S. Taylor, K. H. Burrell, M. S. Chu, E. A. Lazarus, T. H. Osborne, S. J. Thompson, and A. D. Turnbull, *Phys. Rev. Lett.* **75**, 4421 (1995).
- ³⁶G. Knorr, *J. Plasma Phys.* **56**, 391 (1996).
- ³⁷S. Zhu, R. Horiuchi, and T. Sato, *Phys. Rev. E* **51**, 6047 (1995).
- ³⁸E. Hameiri and S. T. Chun, *Phys. Rev. A* **41**, 1186 (1990).
- ³⁹E. Hameiri and H. A. Holties, *Phys. Plasmas* **1**, 3807 (1994).
- ⁴⁰U. Shumlak and C. W. Hartman, *Phys. Rev. Lett.* **75**, 3285 (1995).
- ⁴¹D. Pfirsch and R. N. Sudan, *Phys. Plasmas* **3**, 29 (1996).
- ⁴²R. D. Milroy and J. T. Slough, *Phys. Fluids* **30**, 3566 (1987).